

Measurement of $W\gamma$ and $Z\gamma$ Production in $p\bar{p}$ Collisions at $\sqrt{s} = 1.96$ TeV

D. Acosta,¹⁶ J. Adelman,¹² T. Affolder,⁹ T. Akimoto,⁵⁴ M.G. Albrow,¹⁵ D. Ambrose,⁴³ S. Amerio,⁴² D. Amidei,³³ A. Anastassov,⁵⁰ K. Anikeev,³¹ A. Annovi,⁴⁴ J. Antos,¹ M. Aoki,⁵⁴ G. Apollinari,¹⁵ T. Arisawa,⁵⁶ J.-F. Arguin,³² A. Artikov,¹³ W. Ashmanskas,¹⁵ A. Attal,⁷ F. Azfar,⁴¹ P. Azzi-Bacchetta,⁴² N. Bacchetta,⁴² H. Bachacou,²⁸ W. Badgett,¹⁵ A. Barbaro-Galtieri,²⁸ G.J. Barker,²⁵ V.E. Barnes,⁴⁶ B.A. Barnett,²⁴ S. Baroiant,⁶ M. Barone,¹⁷ G. Bauer,³¹ F. Bedeschi,⁴⁴ S. Behari,²⁴ S. Belforte,⁵³ G. Bellettini,⁴⁴ J. Bellinger,⁵⁸ E. Ben-Haim,¹⁵ D. Benjamin,¹⁴ A. Beretvas,¹⁵ A. Bhatti,⁴⁸ M. Binkley,¹⁵ D. Bisello,⁴² M. Bishai,¹⁵ R.E. Blair,² C. Blocker,⁵ K. Bloom,³³ B. Blumenfeld,²⁴ A. Bocci,⁴⁸ A. Bodek,⁴⁷ G. Bolla,⁴⁶ A. Bolshov,³¹ P.S.L. Booth,²⁹ D. Bortoletto,⁴⁶ J. Boudreau,⁴⁵ S. Bourov,¹⁵ C. Bromberg,³⁴ E. Brubaker,¹² J. Budagov,¹³ H.S. Budd,⁴⁷ K. Burkett,¹⁵ G. Busetto,⁴² P. Bussey,¹⁹ K.L. Byrum,² S. Cabrera,¹⁴ M. Campanelli,¹⁸ M. Campbell,³³ A. Canepa,⁴⁶ M. Casarsa,⁵³ D. Carlsmith,⁵⁸ S. Carron,¹⁴ R. Carosi,⁴⁴ M. Cavalli-Sforza,³ A. Castro,⁴ P. Catastini,⁴⁴ D. Cauz,⁵³ A. Cerri,²⁸ C. Cerri,⁴⁴ L. Cerrito,²³ J. Chapman,³³ C. Chen,⁴³ Y.C. Chen,¹ M. Chertok,⁶ G. Chiarelli,⁴⁴ G. Chlachidze,¹³ F. Chlebana,¹⁵ I. Cho,²⁷ K. Cho,²⁷ D. Chokheli,¹³ M.L. Chu,¹ S. Chuang,⁵⁸ J.Y. Chung,³⁸ W.-H. Chung,⁵⁸ Y.S. Chung,⁴⁷ C.I. Ciobanu,²³ M.A. Ciocci,⁴⁴ A.G. Clark,¹⁸ D. Clark,⁵ M. Coca,⁴⁷ A. Connolly,²⁸ M. Convery,⁴⁸ J. Conway,⁶ B. Cooper,³⁰ M. Cordelli,¹⁷ G. Cortiana,⁴² J. Cranshaw,⁵² J. Cuevas,¹⁰ R. Culbertson,¹⁵ C. Currat,²⁸ D. Cyr,⁵⁸ D. Dagenhart,⁵ S. Da Ronco,⁴² S. D'Auria,¹⁹ P. de Barbaro,⁴⁷ S. De Cecco,⁴⁹ G. De Lentdecker,⁴⁷ S. Dell'Agnello,¹⁷ M. Dell'Orso,⁴⁴ S. Demers,⁴⁷ L. Demortier,⁴⁸ M. Deninno,⁴ D. De Pedis,⁴⁹ P.F. Derwent,¹⁵ C. Dionisi,⁴⁹ J.R. Dittmann,¹⁵ P. Doksus,²³ A. Dominguez,²⁸ S. Donati,⁴⁴ M. Donega,¹⁸ J. Donini,⁴² M. D'Onofrio,¹⁸ T. Dorigo,⁴² V. Drollinger,³⁶ K. Ebina,⁵⁶ N. Eddy,²³ R. Ely,²⁸ R. Erbacher,⁶ M. Erdmann,²⁵ D. Errede,²³ S. Errede,²³ R. Eusebi,⁴⁷ H.-C. Fang,²⁸ S. Farrington,²⁹ I. Fedorko,⁴⁴ R.G. Feild,⁵⁹ M. Feindt,²⁵ J.P. Fernandez,⁴⁶ C. Ferretti,³³ R.D. Field,¹⁶ I. Fiori,⁴⁴ G. Flanagan,³⁴ B. Flaugher,¹⁵ L.R. Flores-Castillo,⁴⁵ A. Foland,²⁰ S. Forrester,⁶ G.W. Foster,¹⁵ M. Franklin,²⁰ J.C. Freeman,²⁸ H. Frisch,¹² Y. Fujii,²⁶ I. Furic,¹² A. Gajjar,²⁹ A. Gallas,³⁷ J. Galyardt,¹¹ M. Gallinaro,⁴⁸ M. Garcia-Sciveres,²⁸ A.F. Garfinkel,⁴⁶ C. Gay,⁵⁹ H. Gerberich,¹⁴ D.W. Gerdes,³³ E. Gerchtein,¹¹ S. Giagu,⁴⁹ P. Giannetti,⁴⁴ A. Gibson,²⁸ K. Gibson,¹¹ C. Ginsburg,⁵⁸ K. Giolo,⁴⁶ M. Giordani,⁵³ G. Giurgiu,¹¹ V. Glagolev,¹³ D. Glenzinski,¹⁵ M. Gold,³⁶ N. Goldschmidt,³³ D. Goldstein,⁷ J. Goldstein,⁴¹ G. Gomez,¹⁰ G. Gomez-Ceballos,³¹ M. Goncharov,⁵¹ O. González,⁴⁶ I. Gorelov,³⁶ A.T. Goshaw,¹⁴ Y. Gotra,⁴⁵ K. Goulianatos,⁴⁸ A. Gresele,⁴ M. Griffiths,²⁹ C. Grossos-Pilcher,¹² U. Grundler,²³ M. Guenther,⁴⁶ J. Guimaraes da Costa,²⁰ C. Haber,²⁸ K. Hahn,⁴³ S.R. Hahn,¹⁵ E. Halkiadakis,⁴⁷ A. Hamilton,³² R. Handler,⁵⁸ F. Happacher,¹⁷ K. Hara,⁵⁴ M. Hare,⁵⁵ R.F. Harr,⁵⁷ R.M. Harris,¹⁵ F. Hartmann,²⁵ K. Hatakeyama,⁴⁸ J. Hauser,⁷ C. Hays,¹⁴ H. Hayward,²⁹ E. Heider,⁵⁵ B. Heinemann,²⁹ J. Heinrich,⁴³ M. Hennecke,²⁵ M. Herndon,²⁴ C. Hill,⁹ D. Hirschbuehl,²⁵ A. Hocker,⁴⁷ K.D. Hoffman,¹² A. Holloway,²⁰ S. Hou,¹ M.A. Houlden,²⁹ B.T. Huffman,⁴¹ Y. Huang,¹⁴ R.E. Hughes,³⁸ J. Huston,³⁴ K. Ikado,⁵⁶ J. Incandela,⁹ G. Introzzi,⁴⁴ M. Iori,⁴⁹ Y. Ishizawa,⁵⁴ C. Issever,⁹ A. Ivanov,⁴⁷ Y. Iwata,²² B. Iyutin,³¹ E. James,¹⁵ D. Jang,⁵⁰ J. Jarrell,³⁶ D. Jeans,⁴⁹ H. Jensen,¹⁵ E.J. Jeon,²⁷ M. Jones,⁴⁶ K.K. Joo,²⁷ S. Jun,¹¹ T. Junk,²³ T. Kamon,⁵¹ J. Kang,³³ M. Karagoz Unel,³⁷ P.E. Karchin,⁵⁷ S. Kartal,¹⁵ Y. Kato,⁴⁰ Y. Kemp,²⁵ R. Kephart,¹⁵ U. Kerzel,²⁵ V. Khotilovich,⁵¹ B. Kilminster,³⁸ D.H. Kim,²⁷ H.S. Kim,²³ J.E. Kim,²⁷ M.J. Kim,¹¹ M.S. Kim,²⁷ S.B. Kim,²⁷ S.H. Kim,⁵⁴ T.H. Kim,³¹ Y.K. Kim,¹² B.T. King,²⁹ M. Kirby,¹⁴ L. Kirsch,⁵ S. Klimenko,¹⁶ B. Knuteson,³¹ B.R. Ko,¹⁴ H. Kobayashi,⁵⁴ P. Koehn,³⁸ D.J. Kong,²⁷ K. Kondo,⁵⁶ J. Konigsberg,¹⁶ K. Kordas,³² A. Korn,³¹ A. Korytov,¹⁶ K. Kotelnikov,³⁵ A.V. Kotwal,¹⁴ A. Kovalev,⁴³ J. Kraus,²³ I. Kravchenko,³¹ A. Kreymer,¹⁵ J. Kroll,⁴³ M. Kruse,¹⁴ V. Krutelyov,⁵¹ S.E. Kuhlmann,² N. Kuznetsova,¹⁵ A.T. Laasanen,⁴⁶ S. Lai,³² S. Lami,⁴⁸ S. Lammel,¹⁵ J. Lancaster,¹⁴ M. Lancaster,³⁰ R. Lander,⁶ K. Lannon,³⁸ A. Lath,⁵⁰ G. Latino,³⁶ R. Lauhakangas,²¹ I. Lazzizzera,⁴² Y. Le,²⁴ C. Lecci,²⁵ T. LeCompte,² J. Lee,²⁷ J. Lee,⁴⁷ S.W. Lee,⁵¹ R. Lefevre,³ N. Leonardo,³¹ S. Leone,⁴⁴ J.D. Lewis,¹⁵ K. Li,⁵⁹ C. Lin,⁵⁹ C.S. Lin,¹⁵ M. Lindgren,¹⁵ T.M. Liss,²³ D.O. Litvintsev,¹⁵ T. Liu,¹⁵ Y. Liu,¹⁸ N.S. Lockyer,⁴³ A. Loginov,³⁵ M. Loretti,⁴² P. Loverre,⁴⁹ R.-S. Lu,¹ D. Lucchesi,⁴² P. Lujan,²⁸ P. Lukens,¹⁵ G. Lungu,¹⁶ L. Lyons,⁴¹ J. Lys,²⁸ R. Lysak,¹ D. MacQueen,³² R. Madrak,²⁰ K. Maeshima,¹⁵ P. Maksimovic,²⁴ L. Malferrari,⁴ G. Manca,²⁹ R. Marginean,³⁸ M. Martin,²⁴ A. Martin,⁵⁹ V. Martin,³⁷ M. Martínez,³ T. Maruyama,⁵⁴ H. Matsunaga,⁵⁴ M. Mattson,⁵⁷ P. Mazzanti,⁴ K.S. McFarland,⁴⁷ D. McGivern,³⁰ P.M. McIntyre,⁵¹ P. McNamara,⁵⁰ R. McNulty,²⁹ S. Menzemer,³¹ A. Menzione,⁴⁴ P. Merkel,¹⁵ C. Mesropian,⁴⁸ A. Messina,⁴⁹ T. Miao,¹⁵ N. Miladinovic,⁵ L. Miller,²⁰ R. Miller,³⁴ J.S. Miller,³³ R. Miquel,²⁸ S. Miscetti,¹⁷ G. Mitselmakher,¹⁶ A. Miyamoto,²⁶ Y. Miyazaki,⁴⁰ N. Moggi,⁴ B. Mohr,⁷ R. Moore,¹⁵ M. Morello,⁴⁴ A. Mukherjee,¹⁵ M. Mulhearn,³¹ T. Muller,²⁵ R. Mumford,²⁴ A. Munar,⁴³ P. Murat,¹⁵ J. Nachtman,¹⁵ S. Nahm,⁵⁹ I. Nakamura,⁴³ I. Nakano,³⁹ A. Napier,⁵⁵ R. Napora,²⁴ D. Naumov,³⁶ V. Necula,¹⁶ F. Niell,³³ J. Nielsen,²⁸ C. Nelson,¹⁵ T. Nelson,¹⁵ C. Neu,⁴³ M.S. Neubauer,⁸ C. Newman-Holmes,¹⁵ A.-S. Nicollerat,¹⁸ T. Nigmanov,⁴⁵ L. Nodulman,² O. Norniella,³ K. Oesterberg,²¹ T. Ogawa,⁵⁶ S.H. Oh,¹⁴ Y.D. Oh,²⁷ T. Ohsugi,²² T. Okusawa,⁴⁰ R. Oldeman,⁴⁹ R. Orava,²¹ W. Orejudos,²⁸ C. Pagliarone,⁴⁴ F. Palmonari,⁴⁴ R. Paoletti,⁴⁴ V. Papadimitriou,¹⁵

S. Pashapour,³² J. Patrick,¹⁵ G. Pauletta,⁵³ M. Paulini,¹¹ T. Pauly,⁴¹ C. Paus,³¹ D. Pellett,⁶ A. Penzo,⁵³ T.J. Phillips,¹⁴ G. Piacentino,⁴⁴ J. Piedra,¹⁰ K.T. Pitts,²³ C. Plager,⁷ A. Pompos,⁴⁶ L. Pondrom,⁵⁸ G. Pope,⁴⁵ O. Poukhov,¹³ F. Prakoshyn,¹³ T. Pratt,²⁹ A. Pronko,¹⁶ J. Proudfoot,² F. Ptahos,¹⁷ G. Punzi,⁴⁴ J. Rademacker,⁴¹ A. Rakitine,³¹ S. Rappoccio,²⁰ F. Ratnikov,⁵⁰ H. Ray,³³ A. Reichold,⁴¹ B. Reisert,¹⁵ V. Rekovic,³⁶ P. Renton,⁴¹ M. Rescigno,⁴⁹ F. Rimondi,⁴ K. Rinnert,²⁵ L. Ristori,⁴⁴ W.J. Robertson,¹⁴ A. Robson,⁴¹ T. Rodrigo,¹⁰ S. Rolli,⁵⁵ L. Rosenson,³¹ R. Roser,¹⁵ R. Rossin,⁴² C. Rott,⁴⁶ J. Russ,¹¹ A. Ruiz,¹⁰ D. Ryan,⁵⁵ H. Saarikko,²¹ S. Sabik,³² A. Safonov,⁶ R. St. Denis,¹⁹ W.K. Sakumoto,⁴⁷ G. Salamanna,⁴⁹ D. Saltzberg,⁷ C. Sanchez,³ A. Sansoni,¹⁷ L. Santi,⁵³ S. Sarkar,⁴⁹ K. Sato,⁵⁴ P. Savard,³² A. Savoy-Navarro,¹⁵ P. Schlabach,¹⁵ E.E. Schmidt,¹⁵ M.P. Schmidt,⁵⁹ M. Schmitt,³⁷ L. Scodellaro,⁴² A. Scribano,⁴⁴ F. Scuri,⁴⁴ A. Sedov,⁴⁶ S. Seidel,³⁶ Y. Seiya,⁴⁰ F. Semeria,⁴ L. Sexton-Kennedy,¹⁵ I. Sfiligoi,¹⁷ M.D. Shapiro,²⁸ T. Shears,²⁹ P.F. Shepard,⁴⁵ M. Shimojima,⁵⁴ M. Shochet,¹² Y. Shon,⁵⁸ I. Shreyber,³⁵ A. Sidoti,⁴⁴ J. Siegrist,²⁸ M. Siket,¹ A. Sill,⁵² P. Sinervo,³² A. Sisakyan,¹³ A. Skiba,²⁵ A.J. Slaughter,¹⁵ K. Sliwa,⁵⁵ D. Smirnov,³⁶ J.R. Smith,⁶ F.D. Snider,¹⁵ R. Snihur,³² S.V. Somalwar,⁵⁰ J. Spalding,¹⁵ M. Spezziga,⁵² L. Spiegel,¹⁵ F. Spinella,⁴⁴ M. Spiropulu,⁹ P. Squillacioti,⁴⁴ H. Stadie,²⁵ A. Stefanini,⁴⁴ B. Stelzer,³² O. Stelzer-Chilton,³² J. Strologas,³⁶ D. Stuart,⁹ A. Sukhanov,¹⁶ K. Sumorok,³¹ H. Sun,⁵⁵ T. Suzuki,⁵⁴ A. Taffard,²³ R. Tafirout,³² S.F. Takach,⁵⁷ H. Takano,⁵⁴ R. Takashima,²² Y. Takeuchi,⁵⁴ K. Takikawa,⁵⁴ M. Tanaka,² R. Tanaka,³⁹ N. Tanimoto,³⁹ S. Tapprogge,²¹ M. Tecchio,³³ P.K. Teng,¹ K. Terashi,⁴⁸ R.J. Tesarek,¹⁵ S. Tether,³¹ J. Thom,¹⁵ A.S. Thompson,¹⁹ E. Thomson,⁴³ P. Tipton,⁴⁷ V. Tiwari,¹¹ S. Tkaczyk,¹⁵ D. Toback,⁵¹ K. Tollefson,³⁴ T. Tomura,⁵⁴ D. Tonelli,⁴⁴ M. Tönnesmann,³⁴ S. Torre,⁴⁴ D. Torretta,¹⁵ S. Tourneur,¹⁵ W. Trischuk,³² J. Tseng,⁴¹ R. Tsuchiya,⁵⁶ S. Tsuno,³⁹ D. Tsybychev,¹⁶ N. Turini,⁴⁴ M. Turner,²⁹ F. Ukegawa,⁵⁴ T. Unverhau,¹⁹ S. Uozumi,⁵⁴ D. Usynin,⁴³ L. Vacavant,²⁸ A. Vaiciulis,⁴⁷ A. Varganov,³³ E. Vataga,⁴⁴ S. Vejcik III,¹⁵ G. Velev,¹⁵ V. Veszpremi,⁴⁶ G. Veramendi,²³ T. Vickey,²³ R. Vidal,¹⁵ I. Vila,¹⁰ R. Vilar,¹⁰ I. Vollrath,³² I. Vollobouev,²⁸ M. von der Mey,⁷ P. Wagner,⁵¹ R.G. Wagner,² R.L. Wagner,¹⁵ W. Wagner,²⁵ R. Wallny,⁷ T. Walter,²⁵ T. Yamashita,³⁹ K. Yamamoto,⁴⁰ Z. Wan,⁵⁰ M.J. Wang,¹ S.M. Wang,¹⁶ A. Warburton,³² B. Ward,¹⁹ S. Waschke,¹⁹ D. Waters,³⁰ T. Watts,⁵⁰ M. Weber,²⁸ W.C. Wester III,¹⁵ B. Whitehouse,⁵⁵ A.B. Wicklund,² E. Wicklund,¹⁵ H.H. Williams,⁴³ P. Wilson,¹⁵ B.L. Winer,³⁸ P. Wittich,⁴³ S. Wolbers,¹⁵ M. Wolter,⁵⁵ M. Worcester,⁷ S. Worm,⁵⁰ T. Wright,³³ X. Wu,¹⁸ F. Würthwein,⁸ A. Wyatt,³⁰ A. Yagil,¹⁵ U.K. Yang,¹² W. Yao,²⁸ G.P. Yeh,¹⁵ K. Yi,²⁴ J. Yoh,¹⁵ P. Yoon,⁴⁷ K. Yorita,⁵⁶ T. Yoshida,⁴⁰ I. Yu,²⁷ S. Yu,⁴³ Z. Yu,⁵⁹ J.C. Yun,¹⁵ L. Zanello,⁴⁹ A. Zanetti,⁵³ I. Zaw,²⁰ F. Zetti,⁴⁴ J. Zhou,⁵⁰ A. Zsenei,¹⁸ and S. Zucchelli,⁴

(CDF Collaboration)

¹ Institute of Physics, Academia Sinica, Taipei, Taiwan 11529, Republic of China

² Argonne National Laboratory, Argonne, Illinois 60439

³ Institut de Fisica d'Altes Energies, Universitat Autonoma de Barcelona, E-08193, Bellaterra (Barcelona), Spain

⁴ Istituto Nazionale di Fisica Nucleare, University of Bologna, I-40127 Bologna, Italy

⁵ Brandeis University, Waltham, Massachusetts 02254

⁶ University of California at Davis, Davis, California 95616

⁷ University of California at Los Angeles, Los Angeles, California 90024

⁸ University of California at San Diego, La Jolla, California 92093

⁹ University of California at Santa Barbara, Santa Barbara, California 93106

¹⁰ Instituto de Fisica de Cantabria, CSIC-University of Cantabria, 39005 Santander, Spain

¹¹ Carnegie Mellon University, Pittsburgh, PA 15213

¹² Enrico Fermi Institute, University of Chicago, Chicago, Illinois 60637

¹³ Joint Institute for Nuclear Research, RU-141980 Dubna, Russia

¹⁴ Duke University, Durham, North Carolina 27708

¹⁵ Fermi National Accelerator Laboratory, Batavia, Illinois 60510

¹⁶ University of Florida, Gainesville, Florida 32611

¹⁷ Laboratori Nazionali di Frascati, Istituto Nazionale di Fisica Nucleare, I-00044 Frascati, Italy

¹⁸ University of Geneva, CH-1211 Geneva 4, Switzerland

¹⁹ Glasgow University, Glasgow G12 8QQ, United Kingdom

²⁰ Harvard University, Cambridge, Massachusetts 02138

²¹ The Helsinki Group: Helsinki Institute of Physics; and Division of High Energy Physics, Department of Physical Sciences, University of Helsinki, FIN-00044, Helsinki, Finland

²² Hiroshima University, Higashi-Hiroshima 724, Japan

²³ University of Illinois, Urbana, Illinois 61801

²⁴ The Johns Hopkins University, Baltimore, Maryland 21218

²⁵ Institut für Experimentelle Kernphysik, Universität Karlsruhe, 76128 Karlsruhe, Germany

²⁶ High Energy Accelerator Research Organization (KEK), Tsukuba, Ibaraki 305, Japan

²⁷ Center for High Energy Physics: Kyungpook National University, Taegu 702-701; Seoul National University, Seoul 151-742; and SungKyunKwan University, Suwon 440-746; Korea

²⁸ Ernest Orlando Lawrence Berkeley National Laboratory, Berkeley, California 94720

²⁹ University of Liverpool, Liverpool L69 7ZE, United Kingdom

³⁰ University College London, London WC1E 6BT, United Kingdom

³¹ Massachusetts Institute of Technology, Cambridge, Massachusetts 02139

³² Institute of Particle Physics: McGill University, Montréal, Canada H3A 2T8; and University of Toronto, Toronto, Canada M5S 1A7

³³ University of Michigan, Ann Arbor, Michigan 48109

³⁴ Michigan State University, East Lansing, Michigan 48824

³⁵ Institution for Theoretical and Experimental Physics, ITEP, Moscow 117259, Russia

³⁶ University of New Mexico, Albuquerque, New Mexico 87131

³⁷ Northwestern University, Evanston, Illinois 60208

³⁸ The Ohio State University, Columbus, Ohio 43210

³⁹ Okayama University, Okayama 700-8530, Japan

⁴⁰ Osaka City University, Osaka 588, Japan

⁴¹ University of Oxford, Oxford OX1 3RH, United Kingdom

⁴² University of Padova, Istituto Nazionale di Fisica Nucleare, Sezione di Padova-Trento, I-35131 Padova, Italy

⁴³ University of Pennsylvania, Philadelphia, Pennsylvania 19104

⁴⁴ Istituto Nazionale di Fisica Nucleare, University and Scuola Normale Superiore of Pisa, I-56100 Pisa, Italy

⁴⁵ University of Pittsburgh, Pittsburgh, Pennsylvania 15260

⁴⁶ Purdue University, West Lafayette, Indiana 47907

⁴⁷ University of Rochester, Rochester, New York 14627

⁴⁸ The Rockefeller University, New York, New York 10021

⁴⁹ Istituto Nazionale di Fisica Nucleare, Sezione di Roma 1, University di Roma "La Sapienza," I-00185 Roma, Italy

⁵⁰ Rutgers University, Piscataway, New Jersey 08855

⁵¹ Texas A&M University, College Station, Texas 77843

⁵² Texas Tech University, Lubbock, Texas 79409

⁵³ Istituto Nazionale di Fisica Nucleare, University of Trieste/ Udine, Italy

⁵⁴ University of Tsukuba, Tsukuba, Ibaraki 305, Japan

⁵⁵ Tufts University, Medford, Massachusetts 02155

⁵⁶ Waseda University, Tokyo 169, Japan

⁵⁷ Wayne State University, Detroit, Michigan 48201

⁵⁸ University of Wisconsin, Madison, Wisconsin 53706

⁵⁹ Yale University, New Haven, Connecticut 06520

The Standard Model predictions for $W\gamma$ and $Z\gamma$ production are tested using an integrated luminosity of 200 pb^{-1} of $p\bar{p}$ collision data collected at the Collider Detector at Fermilab. The cross sections are measured by selecting leptonic decays of the W and Z bosons, and photons with transverse energy $E_T > 7 \text{ GeV}$ that are well separated from leptons. The production cross sections and kinematic distributions for the $W\gamma$ and $Z\gamma$ data are compared to SM predictions.

The study of the characteristics of $W\gamma$ and $Z\gamma$ production is an important test of the Standard Model (SM) description of gauge boson interactions and is sensitive to physics beyond the SM. The $W\gamma$ and $Z\gamma$ cross sections are directly sensitive to the trilinear gauge couplings which are uniquely predicted by the non-Abelian gauge group of the SM electroweak sector $SU(2)_L \times U(1)_Y$. $W\gamma$ production can be used to study the $WW\gamma$ vertex and $Z\gamma$ production can be used to constrain the $ZZ\gamma$ and $Z\gamma\gamma$ vertices which vanish in the SM [1–3]. Physics beyond the SM (e.g. compositeness models or excited W or Z bosons) could alter the cross sections and the production kinematics. $W\gamma$ and $Z\gamma$ production are also important background contributions to searches for new physics, e.g. in Gauge Mediated Supersymmetry Breaking models [4].

This report presents measurements of $p\bar{p} \rightarrow l\nu\gamma + X$ and $p\bar{p} \rightarrow l^+l^-\gamma + X$ production at $\sqrt{s}=1.96$ TeV at the Tevatron accelerator using data obtained with the upgraded Collider Detector at Fermilab (CDF). In the SM the $l\nu\gamma$ and $l^+l^-\gamma$ final states occur due to $W\gamma \rightarrow l\nu\gamma$ and $Z\gamma \rightarrow l^+l^-\gamma$ production, as well as via lepton bremsstrahlung: $W \rightarrow l\nu \rightarrow l\nu\gamma$ and $Z \rightarrow l^+l^- \rightarrow l^+l^-\gamma$. Throughout this letter the notation “ Z ” is used to specify Z/γ^* production via the Drell-Yan process. The notations $W\gamma$ and $Z\gamma$ are used to denote the $l\nu\gamma$ and $l^+l^-\gamma$ final states.

The data are taken at higher center of mass energy and constitute a larger data sample by at least a factor of two than previous measurements [5–9]. They were collected between March 2002 and September 2003, and correspond to an integrated luminosity of about 200 pb^{-1} . W and Z bosons are selected in their electron and muon decay modes. Additionally, a photon with transverse energy above 7 GeV is selected. The production properties of the $W\gamma$ and $Z\gamma$ events are compared to the SM predictions.

The CDF detector is described in detail elsewhere [10]. Transverse momenta of charged particles (p_T)¹ are measured by an eight-layer silicon strip detector [11] and a 96-layer drift chamber (COT) [12] inside a 1.4 Tesla magnetic field. The COT provides coverage with high efficiency for $|\eta| < 1$. At higher $|\eta|$ the silicon detector is used for measuring charged particles. Electromagnetic

and hadronic calorimeters surround the tracking system. They are segmented in a projective tower geometry and measure energies E of charged and neutral particles in the central ($|\eta| < 1.1$) and forward ($1.1 < |\eta| < 3.6$) regions. Each calorimeter has an electromagnetic shower profile detector positioned at the shower maximum. Located at the inner face of the central calorimeter, the central preradiator chambers use the solenoid coil as a radiator to measure the shower development. These two detectors are used for the photon identification and background determination. The calorimeters are surrounded by muon drift chambers covering $|\eta| < 1$. Gas Cherenkov counters [13] measure the average number of $p\bar{p}$ inelastic collisions per bunch crossing and thereby determine the beam luminosity.

For the W and Z boson selection with decays into muons or central electrons, the trigger is solely based on the identification of a high transverse momentum lepton [14]. For W 's decaying to forward electrons, the trigger additionally requires $\cancel{E}_T > 15 \text{ GeV}$. Offline, a high- p_T lepton ($l = e, \mu$) is required to fulfill tighter selection criteria [14]. Electron candidates are required to have $E_T > 25 \text{ GeV}$ and $|\eta| < 2.6$. In the central region, a COT track with $p_T > 10 \text{ GeV}/c$ must be associated with the energy deposition, while in the forward region calorimeter-seeded silicon tracking is used to associate a track with the electromagnetic shower [15]. The electromagnetic shower profile of an electron candidate must be consistent with expectations from test beam data. Muons are selected by requiring a COT track with $p_T > 20 \text{ GeV}/c$, and the associated energy deposition in the calorimeter to be consistent with that expected for a muon [14]. In addition, for at least one muon per event, the track segments in the muon chambers must match the extrapolated position of the muon track and be in the range $|\eta| < 1.0$. Both electrons and muons must be isolated from other calorimeter energy depositions [14]. The selected samples correspond to an integrated luminosity of 202 pb^{-1} (168 pb^{-1}) for central (forward) electrons and 192 pb^{-1} (175 pb^{-1}) for muons in the region $|\eta| < 0.6$ ($0.6 < |\eta| < 1.0$).

For $W \rightarrow l\nu$ candidates, we also require $\cancel{E}_T > 25$ (20) GeV in the electron (muon) channel as evidence for the neutrino. For the $W \rightarrow \mu\nu$ channel, events with an additional track with $p_T > 10 \text{ GeV}/c$ and a calorimeter signal consistent with a muon, are rejected as potential background from $Z \rightarrow \mu^+\mu^-$. For the selection of Z candidates, a second electron is required in the electron channel and a second isolated track consistent with a minimum ionizing particle in the muon channel.

In the $Z\gamma$ analysis the invariant mass of the dilepton pair, $M(l^+, l^-)$, is required to be in the range $40 < M(l^+, l^-) < 130 \text{ GeV}/c^2$ to enhance the sensitivity to on-shell Z boson production. In the $W\gamma$ analysis the transverse mass, $M_T(l, \cancel{E}_T)$, is required to be in the range $30 < M_T(l, \cancel{E}_T) < 120 \text{ GeV}/c^2$ to select on-shell W bo-

¹We use a cylindrical coordinate system about the beampipe in which θ is the polar angle, ϕ is the azimuthal angle and $\eta = -\ln \tan(\theta/2)$. $E_T = E \sin \theta$ and $p_T = p \sin \theta$ where E is the energy measured by the calorimeter and p the momentum measured in the tracking system. $\vec{\cancel{E}}_T = -\sum_i E_T^i \vec{n}_i$ where \vec{n}_i is a unit vector that points from the interaction vertex to the i th calorimeter tower in the transverse plane. \cancel{E}_T is the magnitude of $\vec{\cancel{E}}_T$. If muons are identified in the event, \cancel{E}_T is corrected for the muon momenta.

son production. The transverse mass is used since the longitudinal component of the neutrino momentum cannot be measured: $M_T(l, \not{E}_T) = \sqrt{2p_T^l \not{E}_T (1 - \cos \phi_{l, \not{E}_T})}$, where ϕ_{l, \not{E}_T} is the difference in azimuthal angle between the lepton momentum and the missing transverse momentum vector.

After reconstructing a W or Z candidate, we select a photon with $E_T^\gamma > 7$ GeV within $|\eta_\gamma| < 1.0$ which is isolated from other particles in both the calorimeter and the tracking detectors. The transverse energy deposit around the photon in a cone $\Delta R = \sqrt{(\eta_i - \eta_\gamma)^2 + (\phi_i - \phi_\gamma)^2} = 0.4$ is required to be less than 10% of the photon transverse energy for $E_T^\gamma < 20$ GeV and less than $2 + 0.02(E_T^\gamma - 20)$ GeV for $E_T^\gamma > 20$ GeV. Here, η_i and ϕ_i denote the location of the energy deposit in the i th calorimeter tower excluding those associated with the photon candidate. The total sum of the track transverse momenta in a cone of 0.4 around the photon candidate is also required to be less than 2 GeV/ c . To remove electron background we require there to be no track with $p_T > 1$ GeV/ c pointing toward the photon candidate. The photon candidate also must have a shower shape consistent with a single particle and must be separated from the lepton by $\Delta R(l, \gamma) = \sqrt{(\eta_l - \eta_\gamma)^2 + (\phi_l - \phi_\gamma)^2} > 0.7$. This last requirement is placed to suppress the contribution from bremsstrahlung photons. After all selection criteria are applied, 323 $W\gamma$ candidates and 71 $Z\gamma$ candidates are found.

The most important source of background to both the $Z\gamma$ and $W\gamma$ analysis is the production of a real Z or W boson and a hadron which is misidentified as a photon. This background is determined using large event samples triggered on jets at several E_T thresholds: 20, 50, 70 and 100 GeV. We measure the fraction of jets in the samples which pass all the photon selection requirements. This fraction is then corrected for prompt photon contamination within the jet samples. Two methods were used to estimate this contamination. For $E_T^\gamma < 40$ GeV, the estimate of the prompt photon contamination exploits the broader shower shape of $\pi^0 \rightarrow \gamma\gamma$ showers compared to prompt γ showers in the electromagnetic shower profile detector [16]. For $E_T^\gamma > 40$ GeV hits in the central pre-radiator chambers are counted. In this method prompt photons are distinguished from meson decays since the probability of a photon conversion in the magnetic coil is higher for π^0 's than for prompt photons [16]. The resulting fake rate for a jet to pass all photon selection cuts is about 0.3% at $E_T = 10$ GeV and decreases exponentially to about 0.07% for $E_T = 25$ GeV.

We obtain the background prediction by applying this fake rate to jets in W and Z events. The background due to events where neither the leptons nor the photon are genuine is implicitly taken into account in the above estimate. In the $W\gamma$ analysis an additional background arises from $Z\gamma$ production where large \not{E}_T is observed

due to an undetected lepton. This background is larger in the muon than in the electron channel due to the smaller muon coverage of the CDF detector. Another source of background is $\tau\nu_\tau\gamma \rightarrow l\nu_l\bar{\nu}_\tau\nu_\tau\gamma$ production. These two backgrounds are determined using the Monte Carlo generators described below. $\tau\tau\gamma$ is found to be a negligible source of background in both analyses.

A summary of the background contributions for the $W\gamma$ analysis is given in Table I. For the $Z\gamma$ analysis, the only background is due to jets mis-identified as photons. For $e\nu\gamma$, the estimated background is 2.8 ± 0.9 events, and for $\mu\nu\gamma$, it is 2.1 ± 0.6 events.

TABLE I. Background event contributions for the $e\nu\gamma$ and $\mu\nu\gamma$ analyses. The combined statistical and systematic uncertainty on the background prediction is also quoted.

	$e\nu\gamma$	$\mu\nu\gamma$
W +jet	59.5 ± 18.1	27.6 ± 7.5
$\tau\nu\gamma$	1.5 ± 0.2	2.3 ± 0.2
$l^+l^-\gamma$	6.3 ± 0.3	17.4 ± 1.0
Total Background	67.3 ± 18.1	47.3 ± 7.6

The $p\bar{p} \rightarrow l\nu\gamma X$ and $p\bar{p} \rightarrow l^+l^-\gamma X$ SM signal predictions are determined using leading order Monte Carlo generators for all three lepton generations. The matrix element generator [2,3] includes initial and final state photon radiation and the $WW\gamma$ vertex diagram. Initial state QCD radiation and hadronization are included using PYTHIA [17]. The parton momentum distribution is modeled with CTEQ5L parton density functions (PDF's) [18]. $\mathcal{O}(\alpha_s)$ QCD corrections [19] to the $W\gamma$ and $Z\gamma$ production cross sections are calculated using CTEQ5M PDF's [18]. These corrections increase the $W\gamma$ ($Z\gamma$) cross section by 33–55% (27–32%) for E_T^γ in the range 10–55 GeV.

The SM cross section for $p\bar{p} \rightarrow l\nu\gamma X$ production for the kinematic region $E_T^\gamma > 7$ GeV and $\Delta R(l, \gamma) > 0.7$ is 19.3 ± 1.4 pb for the W -boson decaying into a single lepton flavor. For the same kinematic region and with the invariant mass of the dilepton pair $M(l^+, l^-) > 40$ GeV/ c^2 , the cross section for $p\bar{p} \rightarrow l^+l^-\gamma X$ production is 4.5 ± 0.3 pb for the Z -boson decaying into a lepton pair of a single flavor. The 7% uncertainty on the cross section due to higher order contributions and uncertainties on the PDF's is evaluated by changing the factorization scale (2%), the renormalization scale (3%) and comparing the predictions made with several PDF's (5%) [20,21].

The observed (N_{obs}) and expected numbers of signal (N_{sig}) and background (N_{bg}) events in the $W\gamma$ and $Z\gamma$ analyses are given in Table II. Both the electron and muon data are in good agreement with expectations. The systematic uncertainties on these measurements include uncertainties on the event selection efficiency and acceptance. The main contributions come from higher order

QCD corrections to the acceptance and the efficiency of the photon selection. The dominant uncertainty on the background is due to the jet fake rate uncertainty. The total systematic uncertainty on the cross sections is 9–14% for the $W\gamma$ and 3% for the $Z\gamma$ cross sections. An additional uncertainty of 6% arises from the luminosity measurement.

TABLE II. Expected and observed numbers of events for $e\nu\gamma$ and $\mu\nu\gamma$, $e^+e^-\gamma$ and $\mu^+\mu^-\gamma$ production. The systematic uncertainties listed for the expected number of events excludes the 7% uncertainty on the theoretical cross section and the 6% uncertainty in luminosity measurement. The product of the acceptance and efficiency, $A \times \epsilon$, and the measured cross sections, $\sigma(l\nu\gamma)$ and $\sigma(l^+l^-\gamma)$, are also listed. The first uncertainty is statistical and the second is systematic. There is a separate error on the luminosity normalization of 1.2 pb for the $W\gamma$ and 0.3 pb for the $Z\gamma$ cross section measurements.

	$e\nu\gamma$	$\mu\nu\gamma$
N_{sig}	126.8 ± 5.8	95.2 ± 4.9
$N_{sig} + N_{bg}$	194.1 ± 19.1	142.4 ± 9.5
N_{obs}	195	128
$A \times \epsilon$	3.3%	2.4%
$\sigma(l\nu\gamma)$ (pb)	$19.4 \pm 2.1 \pm 2.9$	$16.3 \pm 2.3 \pm 1.8$
	$e^+e^-\gamma$	$\mu^+\mu^-\gamma$
N_{sig}	31.3 ± 1.6	33.6 ± 1.5
$N_{sig} + N_{bg}$	34.1 ± 1.8	35.7 ± 1.7
N_{obs}	36	35
$A \times \epsilon$	3.4%	3.7%
$\sigma(l^+l^-\gamma)$ (pb)	$4.8 \pm 0.8 \pm 0.3$	$4.4 \pm 0.8 \pm 0.2$

The cross section $\sigma(l\nu\gamma)$ is measured in the kinematic range $\Delta R(l, \gamma) > 0.7$ and $E_T^\gamma > 7$ GeV with $\sigma = (N_{obs} - N_{bg}) / (A \times \epsilon \times \int \mathcal{L} dt) = (N_{obs} - N_{bg}) / N_{sig} \times \sigma_{SM}$. Here, $\int \mathcal{L} dt$ is the integrated luminosity, A is the acceptance, ϵ is the selection efficiency and σ_{SM} is the SM cross section of the Monte Carlo simulation sample used for estimating the acceptance and number of expected signal events. The resulting cross sections are given in Table II. The measured cross sections are determined for the full W decay phase space, transverse mass range and photon η range using extrapolations based upon the SM expectation [19]. Combining the electron and muon channel, assuming lepton universality, and taking into account correlations of the systematic uncertainties, yields $\sigma(l\nu\gamma) = 18.1 \pm 3.1$ pb. The theoretical prediction for this cross section is 19.3 ± 1.4 pb.

The cross section $\sigma(l^+l^-\gamma)$ is measured in the kinematic range $\Delta R(l, \gamma) > 0.7$, $E_T^\gamma > 7$ GeV and $M(l^+, l^-) > 40$ GeV/c². We follow the same procedure as for the $W\gamma$ analysis and obtain the cross section listed in Table II. The measured cross sections are determined for the full Z decay phase space, dilepton mass range $M(l^+, l^-) > 40$ GeV/c² and photon η range using extrapolations based upon the SM expectation [19]. The combined electron and muon result is $\sigma(l^+l^-\gamma) = 4.6 \pm 0.6$ pb. The theoretical prediction for this cross section is 4.5 ± 0.3 pb.

olations based upon the SM expectation [19]. The combined electron and muon result is $\sigma(l^+l^-\gamma) = 4.6 \pm 0.6$ pb. The theoretical prediction for this cross section is 4.5 ± 0.3 pb.

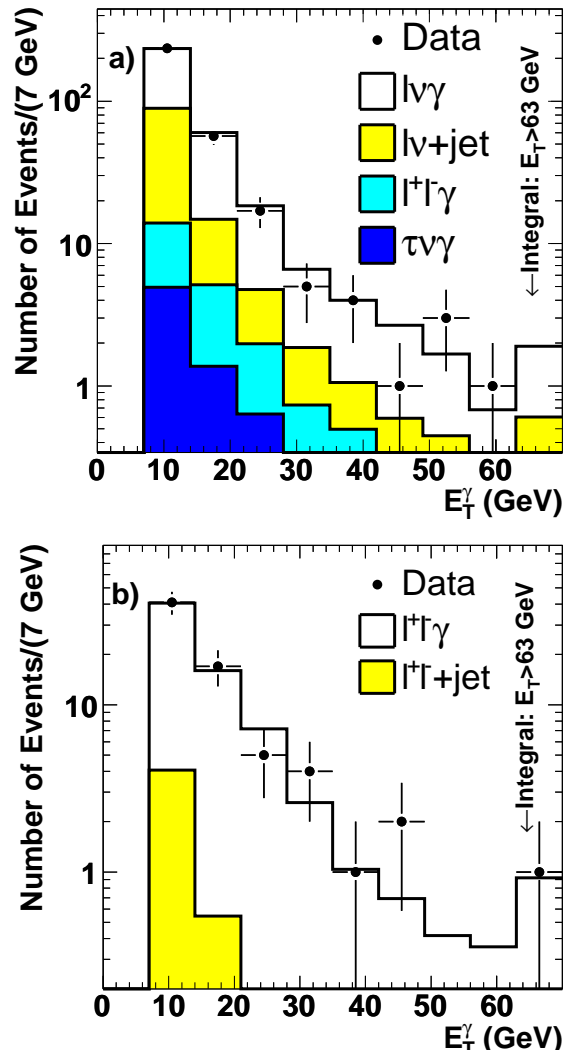


FIG. 1. Photon transverse energy spectrum, E_T^γ , for a) $W\gamma$ and b) $Z\gamma$ candidates selected in the leptonic decay channel. The data are compared with the SM expectations for signal and background with the histograms added cumulatively. In both figures the last bin contains all events with $E_T^\gamma > 63$ GeV.

In addition to these cross section measurements, we compare the SM predictions for several kinematic variables with the data for $E_T^\gamma > 7$ GeV and $\Delta R(l, \gamma) > 0.7$. We choose the E_T^γ and final state mass spectra since these are sensitive tests of SM predictions. The transverse energy of the photon in $W\gamma$ and $Z\gamma$ production is shown in Figure 1. Figure 2 shows the cluster transverse mass [22], $M_T(l\gamma, \nu)$, for $W\gamma$ events and the invariant mass of the (l^+, l^-, γ) system, $M(l^+, l^-, \gamma)$, for $Z\gamma$ events. The data are in good agreement with the SM expectations for both processes. The event with the highest E_T photon, ob-

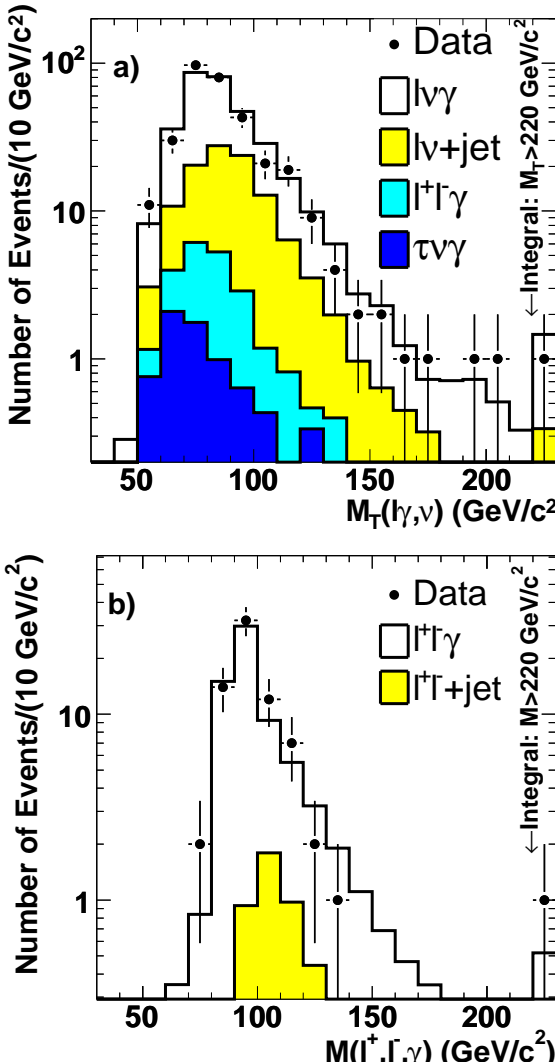


FIG. 2. a) The cluster transverse mass of the lepton-photon-missing E_T system for $W\gamma$ candidates, and b) the invariant mass of the lepton-lepton-photon system for $Z\gamma$ candidates. The data are compared with the SM expectations for signal and background with the histograms added cumulatively. In both figures the last bin contains all events with masses above $220 \text{ GeV}/c^2$.

served in the $e^+e^-\gamma$ channel with $E_T^\gamma = 141 \text{ GeV}$ and $M(e^+, e^-, \gamma) = 382 \text{ GeV}/c^2$, is consistent with the rate expected from SM predictions.

In summary, we have measured $W\gamma$ and $Z\gamma$ production in $p\bar{p}$ collisions at $\sqrt{s} = 1.96 \text{ TeV}$ using data from the CDF experiment. The cross sections, measured to a precision of 15%, are compared to electroweak predictions having an estimated uncertainty of 7%. For E_T^γ above 7 GeV and $\Delta R(l, \gamma) > 0.7$, the production cross sections, and the photon and W/Z boson production kinematics, are found to agree with SM predictions.

Acknowledgments

We thank the Fermilab staff and the technical staffs of

the participating institutions for their vital contributions. We also thank Ulrich Baur for his help and input toward the understanding of theoretical aspects of this analysis.

This work was supported by the U.S. Department of Energy and National Science Foundation; the Italian Istituto Nazionale di Fisica Nucleare; the Ministry of Education, Culture, Sports, Science and Technology of Japan; the Natural Sciences and Engineering Research Council of Canada; the National Science Council of the Republic of China; the Swiss National Science Foundation; the A.P. Sloan Foundation; the Bundesministerium für Bildung und Forschung, Germany; the Korean Science and Engineering Foundation and the Korean Research Foundation; the Particle Physics and Astronomy Research Council and the Royal Society, UK; the Russian Foundation for Basic Research; the Comisión Interministerial de Ciencia y Tecnología, Spain; and in part by the European Community's Human Potential Programme under contract HPRN-CT-20002, Probe for New Physics.

-
- [1] for a review see J. Ellison, J. Wudka, Ann. Rev. Nucl. Part. Sci. **48**, 1-31 (1998)
 - [2] U. Baur and E.L. Berger, Phys. Rev. D **41**, 1476 (1990).
 - [3] U. Baur and E.L. Berger, Phys. Rev. D **47**, 4889 (1993).
 - [4] S. Dimopoulos *et al.* Nucl. Phys. **B488**, 39 (1997); S. Ambrosanio *et al.*, Phys. Rev. D **56**, 1761 (1997); G. F. Giudice, R. Ratazzi, Phys. Rept. **322**, 419 (1999); S. Ambrosanio *et al.*, Phys. Rev. D **55**, 1372 (1997).
 - [5] B. Abbott *et al.*, The D0 Collaboration, Phys. Rev. D **60**, 072002 (1999).
 - [6] S. Abachi *et al.*, The D0 Collaboration, Phys. Rev. Lett. **78**, 3634 (1997).
 - [7] B. Abbott *et al.*, The D0 Collaboration, Phys. Rev. D **57**, 3817 (1998).
 - [8] F. Abe *et al.*, The CDF Collaboration, Phys. Rev. Lett. **74**, 1936 (1995).
 - [9] F. Abe *et al.*, The CDF Collaboration, Phys. Rev. Lett. **74**, 1941 (1995).
 - [10] The CDF Collaboration, FERMILAB-PUB-96-390-E.
 - [11] A. Sill *et al.*, Nucl. Instrum. Methods Phys. Res., Sect. A **447**, 1 (2000).
 - [12] T. Affolder *et al.*, The CDF Collaboration, FERMILAB-PUB-03-355-E, submitted to Nucl. Instrum. Methods Phys. Res., Sect. A.
 - [13] D. Acosta *et al.*, Nucl. Instrum. Methods Phys. Res., Sect. A **461**, 540 (2001).
 - [14] T. Affolder *et al.*, The CDF Collaboration, preprint hep-ex/0406078, accepted by Phys. Rev. Lett.
 - [15] C. Issever, AIP Conf. Proc. **670**, 371 (2001).
 - [16] F. Abe *et al.*, The CDF Collaboration, Phys. Rev. D **48**, 2998 (1993).
 - [17] L. Lönnblad *et al.*, LU-TP 01-21, hep-ph/0108264.
 - [18] H.L. Lai *et al.*, Eur. Phys. J. C **12**, 375 (2000).
 - [19] U. Baur, T. Han and J. Ohnemus, Phys. Rev. D **48**, 5140

- (1993); U. Baur, T. Han and J. Ohnemus, Phys. Rev. D **57**, 2823 (1998).
[20] J. Huston *et al.*, JHEP **07**, 012 (2002).
[21] A. D. Martin *et al.*, Eur. Phys. J. C**23**, 73 (2002).
[22] E.L. Berger, Phys. Lett. **140B**, 259 (1984).